Alexandria Engineering Journal (2020) 59, 1637–1648

HOSTED BY

Alexandria University

Alexandria Engineering Journal

www.elsevier.com/locate/aej
www.sciencedirect.com

Modified eucalyptus bark as a sorbent for simultaneous removal of COD, oil, and Cr(III) from industrial wastewater

Sri Martini [a,b,*], Sharmeen Afroze [b], Kiagus Ahmad Roni [a]

[a] Faculty of Engineering, Chemical Engineering Department, University of Muhammadiyah Palembang, 13 Ulu Palembang, Indonesia
[b] Department of Chemical and Petroleum Engineering, Curtin University, GPO Box U1987, Perth, WA 6845, Australia

Received 4 December 2019; revised 3 April 2020; accepted 10 April 2020
Available online 4 June 2020

KEYWORDS

Adsorption;
COD;
Oil;
Cr(III);
Eucalyptus bark;
Isotherm models

Abstract This study has investigated the efficiency of eucalyptus bark (EB) to remove COD, oil, and Cr(III) from raw petroleum refinery effluent. Experimental works were conducted to assess the performance of raw and modified EB using chemical impregnation, carbonization, and hybrid pre-treatment. Then modified EB by hybrid H_3PO_4/carbonization that showed the best performance was further examined under different operating conditions: namely contact time, solution pH, temperature, and sorbent dosage. In general, removal efficiencies of COD, oil, and Cr(III) increased with the increase in contact time and sorbent dosage while acidic pH was favourable for achieving higher removal efficiency for targeted pollutants. The maximum removal efficiencies of COD, oil, and Cr(III) were 80, 91, and 61%, respectively. Meanwhile, the optimum operating conditions were found at contact time 100 min, sorbent dosage 10 g/L, pH 3, and temperature 25 °C. FTIR and SEM were also applied to characterize the sorbent. The Freundlich adsorption isotherm model shows a better correlation coefficient among the other isotherm models including Langmuir and Dubinin-Radushkevich with the R^2 value of 0.9758. The adsorption kinetic examined using different kinetic models including pseudo-first order, pseudo-second order, intra-particle diffusion, liquid film diffusion, and double exponential follows intra-particle diffusion model.

1. Introduction

Industrial oily effluents which are generated in various industries including petroleum refinery effluent (PRE) contain COD, oil forms, and heavy metals contaminations that need to be removed before the water can be reused for other purposes or discharged into open water system [1,2]. As parts of major pollutants in PRE, COD and oil content must be adjusted to fulfil the allowable standard values stated by regulation when the effluent is disposed to the environment as it can cause adverse effect on aquatic organisms and human health [3,4]. However, removing the emulsified oil is more challenging due to its stability in the aqueous phase [5].

Another threatening content in raw PRE is heavy metals which have toxic effect both in elemental and soluble forms.

* Corresponding author.
E-mail address: s.puaddahtan@graduate.curtin.edu.au (S. Martini).
Peer review under responsibility of Faculty of Engineering, Alexandria University.

https://doi.org/10.1016/j.aej.2020.04.010

Unlike organic pollutants, metals in wastewater cannot be degraded through biological processes. Hence, the eradication of toxic metals such as chromium from industrial effluents is challenging and important to be conducted to avoid further damage of environment condition and disastrous effect on human health as remaining metal ions in open water and contaminated food are responsible for poisoning, cancer, and brain damage [6,7].

Assorted methods including advanced oxidation processes, membrane filtration, and biologically activated sludge have been investigated in order to mitigate various hazardous pollutants including COD, oil, and metal ions in PRE [8–11]. However, the demanding drawbacks of these methods are high operational and maintenance costs, generation of toxic sludge and complicated procedure [3]. Comparatively, adsorption has been found to be an efficient and economic due to its relatively lower processing cost and simple design [12].

Adsorption materials are generally categorized into three main types; inorganics mineral, synthetic organic, and organic sorbents. Inorganic materials such as vermiculite and graphite are leaning toward poorer buoyancy and oil removal efficiency, while commercially available synthetic organic sorbents such as polypropylene might cause detrimental environment issues after their usage [13]. Therefore, compared to others, the use of organic materials or biosorbents from agricultural and plant wastes offers more advantages such as low-cost sorbent, good removal percentage, and environmentally friendly solution for oily waste disposal problems [14–17]. There are varying biodegradable plant-based sorbents which were examined and reported as potential effective sorbents to adsorb oil content such as sago bark, cotton grass, corn stalk, banana peel, barley straw, bagasse, and rice husk [18–21]. In addition, the use of biosorbents was also investigated to degrade COD and some detrimental heavy metals in synthetic or raw industrial effluents such as date pits, sultone, lentil husk, cashew nut, rice husk, palm leaf, and water hyacinth [4,7,22–24].

However, some organic sorbents were also found to show poor oil, metals, and other pollutants removal efficiencies in their raw forms. Then several initial modifications have attempted to bolster the efficiency such as esterification process [25], cellulose enzymes [17], acylation and thermal modifications [26,27] or impregnation method using certain salts and surfactants [14,20,28].

Accordingly, it is worth to investigate and modify other organic materials as a sorbent to treat raw industrial wastewaters including PRE. Eucalyptus trees are fast growing and ubiquitously available in Australia generating huge amounts of its barks in which they are disposed as waste. Even though literature shows that eucalyptus bark (EB) has been examined as the sorbent for cationic dyes and certain heavy metals removal from mostly synthetic aqueous solutions or other industrial wastewaters [29–35], to the best of our knowledge, there are limited or no known reported studies of its potential use for COD, oil and Cr(III) removals from raw PRE.

Therefore, this research was undertaken to explore the efficiency of raw and modified EB for COD, oil, and Cr(III) removals in raw PRE simultaneously. The effectiveness of varying modifications such as carbonization, chemical treatment using various chemical solutions, and hybrid treatment mode was also compared in order to obtain better efficacy of EB to reduce the concentration of selected pollutants. Then the use of modified eucalyptus bark (MEB) showing best performance in preliminary experiment was further implemented under different operating conditions to evaluate the effect of contact time, pH, temperature, and adsorbent dosage on the removal efficiency of targeted pollutants. The effect of rinsing method on the regeneration of saturated MEB using water and different salt solutions was also studied. The adsorption equilibrium data were then analyzed using Langmuir, Freundlich, and Dubinin-Radushkevich models. Besides, adsorption kinetics and thermodynamic parameters were studied to explain the diffusion mode of selected adsorbate in the pores and process feasibility.

2. Materials and methods

2.1. Raw PRE and chemical reagents

Raw PRE was collected from the outlet of the DAF unit of the British Petroleum Kwinana Oil Refinery, Western Australia, prior to biological treatment. Before characterization, the effluent sample was filtered to remove solid particles greater than a millimetre in size. The characteristics of filtered PRE are shown in Table 1. All the samples were stored at 4 °C before use in order to minimize its physical-chemical condition deterioration.

All reagents used were of analytical reagent grade. The pH of the solutions was adjusted by adding either 0.1 M HCl or 0.1 M NaOH solutions. All sample bottles and glass wares were cleaned, rinsed with deionized water, and then oven-dried at 60 °C.

2.2. Adsorbent preparation

Eucalyptus barks (EB) was collected from yard environment of Curtin University –Bentley Campus, Western Australia. The EB material were washed several times with distilled water to remove any impurities and dried at 105 °C for 24 h in a laboratory oven. Then it was crushed by a mechanical grinder (RETSCH, GmbH & Co. KG, West Germany) to obtain powder form then passed through British Standard Sieves (BSS) of 106 μm. Fig. 1 shows the biosorbent appearance before and after initial preparation.

Furthermore, EB biomass was chemically modified by soaking a known amount of the biosorbent in separately selected chemical solutions namely; $ZnCl_2$, NaOH, and H_3PO_4 which have 0.1 M of concentration. The suspensions were shaken on the orbital shaker at 200 rpm at room temperature for 24 hr. Ultimately, biosorbent was further separated

Table 1 Characteristics of raw PRE used in this work.

Parameter	PRE
COD	900
Oil	300
pH	9.5
Cr(III)	1.115
TDS	1300

*Concentrations in mg/L, except pH.

Fig. 1 Raw eucalyptus bark material (a) before and (b) after initial preparation.

from chemical solution and rinsed with deionized water, then it was dried in an oven at 60 °C overnight.

Carbonization modification was conducted by putting the raw biosorbent in a closed tube having a small hole in the top for venting gases produced during carbonization process. The tube was heated in a laboratory muffle furnace to 400 °C and maintained at the selected temperature for 1 h then left to cool to room temperature.

Thus hybrid modification was performed by initially conducting chemical treatment for raw biosorbent followed by carbonization process. All raw and modified sorbents were then stored in the separate airtight plastic containers and were used for conducting adsorption experiments.

2.3. Adsorption experimental and analytical procedures

Raw PRE was measured using a measuring cylinder, then poured into a glass screw cap bottle through a glass filter funnel. Measured biosorbent was added to the bottle. Then the wastewater sample bottles with sorbent were shaken in a Thermo Line Scientific Orbital Incubator at a speed of 200 rpm at decided temperature. After designed contact time, the liquid was withdrawn from the shaker, filtered, and analyzed for its COD, oil, and Cr(III) contents. The effects of selected operating parameters such as contact time (10, 30, 50, 70, 100, 150, 180, and 200 min), initial solution pH (3, 5, 7, 9 and 10), temperature (25, 30, 35, 40, and 45 °C), and adsorbent dosage (5, 10, 15, 20, and 25 g/L) were thoroughly investigated.

Surface morphology and infrared spectrum of the sorbent were characterized by a JEOL 6400 field emission scanning electron microscope (SEM) and a PerkinElmer Spectrum 100 spectrophotometer, respectively.

A HACH DRB200 reactor, DR890 colorimeter, and HACH COD reagent vials with HR 0–1500 mg/L, purchased from Rowe scientific, Australia, were used to measure COD concentration based on the procedure handbook provided (standard method 5220 D) [36].

The oil concentration was measured by a gravimetric method. Raw PRE (20 mL) was transferred to a separating funnel. Then few drops of sulphuric acid (H_2SO_4) solution were added to obtain pH 2.0 before adding 3 mL of n-hexane. The separating funnel was mechanically shaken for 2 min and left to form two separate layers. Then 10 g of anhydrous sodium sulphate (Na_2SO_4) was put on Whatman filter paper of 180 mm that covered the weighed round bottomed flask mouth. The oil layer was collected onto the round bottomed flask. Furthermore, the hexane in oil was separated using rotary evaporator (Butchi Rotavapor R-210 series). Oil sample in the round flask was dried at 103 °C for 15 min and then cooled to room temperature in the desiccator.

The concentration of Cr(III) was determined using a Shimadzu flame model AA-7000 machine of Atomic Absorption Spectrophotometry (AAS) with standard solution and operation set by the manufacture.

The values of COD, oil, and Cr(III) removal efficiencies were determined based on the following equations [37].

$$\text{Removal efficiency}(\%) = \frac{C_0 - C_e}{C_0} \text{x} 100\% \quad (1)$$

where $C_0$and $C_e$are the initial and final concentration (mg/L) in raw PRE, respectively.

2.4. Regeneration study

Regeneration study was also performed to investigate the performance of the sorbent regarding its efficiency to remove adsorbed pollutant from PRE after certain number of cycle. This analysis was done by placing 5 g/L of sorbent in PRE. The mixture was digitally shaken for 60 min at 200 rpm speed. The mixture was then separated by filtering the filtrate for further analysis. The used sorbent was drained for 30 min before starting the next adsorption cycle. Targeted pollutant removal efficiency was recorded and calculated for each cycle.

2.5. Adsorption isotherm models

Three reliable isotherm models; namely Langmuir, Freundlich, and Dubinin-Radushkevich were applied to understand the mechanism of selected pollutant removal during the adsorption process related to the way of adsorbate particles distribution between solid and liquid phase [23]. In this section, the

experimental data of Cr(III) was chosen for both isotherm and kinetic analysis. Further, the correlation coefficient, R^2, was used as a parameter of isotherm model applicability and the results are figured in Figs. 11–13 as well as tabulated in Table 3.

2.5.1. Freundlich isotherm model

This model assumes that the adsorption process occurs on the heterogeneous surface as formulated in Eq. (2) [38,39].

$$\ln q_e = lnk_f + \frac{1}{n}(\ln C_e) \tag{2}$$

where q_e, C_e, k_f, and n are the amount of Cr(III) ions adsorbed per unit of adsorbent at equilibrium time (mg/g), the equilibrium Cr(III) concentration in the solution (mg/L), isotherm constant (mg/g), and the adsorption intensity (g/L), respectively.

2.5.2. Langmuir isotherm model

This model describes that the adsorption takes place onto an ideal homogeneous uniform surface with all sites on the adsorbent surface being equivalent and stated in general linearized Langmuir isotherm as below [38].

$$\frac{C_e}{q_e} = \left(\frac{1}{K_L q_m}\right) + \frac{C_e}{q_m} \tag{3}$$

where q_m and K_L are the values of maximum adsorption capacity (mg/g) and Langmuir constant (L/g) related to adsorption energy (L/mg) which is predicted by plotting $\frac{C_e}{q_e}$ vs C_e.

2.5.3. Dubinin-Radushkevich isotherm model

This model indicates the adsorption mechanism related to Gaussian energy distribution onto a heterogeneous surface. The linearized form of this model is expressed as follows [40].

$$lnq_e = lnq_m - ß\varepsilon^2 \tag{4}$$

where ß and ε are a constant related to adsorption energy and the Polanyi potential related to the equilibrium concentration, respectively. The value of ε can be obtained from Eq. (5) which is stated below.

$$\varepsilon = RTln\left(1 + \frac{1}{C_e}\right) \tag{5}$$

where R is the gas constant (8.314 J/mol K) and T is the absolute temperature (K).

2.6. Adsorption kinetic modelling

Numerous kinetic models including pseudo-first order, pseudo-second order, intra particle diffusion, liquid film diffusion, and double exponential models were applied to study kinetic performance of targeted pollutant adsorption on hybrid MEB sorbent.

2.6.1. Pseudo-first order

Pseudo-first order kinetic model can be linearized in an integral form (Eq. (6)) [38,39,41,42].

$$\log(q_e - q_t) = \log(q_e) - \frac{K_1}{2.303}t \tag{6}$$

where q_t, K_1,and t are pollutants adsorbed at specific time (mg/g), equilibrium rate constant of pseudo first order adsorption (min^{-1}), and time (min), respectively. The adsorption rate constant, K_1, can be calculated from the plot of log (q_e−q_t) vs t.

2.6.2. Pseudo-second order

The pseudo-second order kinetic model can be linearized as following [43,44].

$$\frac{t}{q_t} = \frac{1}{K_2 q_e^2} + \frac{1}{q_e}t \tag{7}$$

where K_2 is the pseudo-second order rate constant (g/mg min) that can be estimated by plotting $\frac{t}{q_t}$ vs t. Thus the constant K_2 can be used to obtain the initial sorption rate (h) at $t = 0$, as follows.

$$h = k_2 q_e^2 \tag{8}$$

The values of k_2, h, and q_e can be calculated by the plot of t/q vs t.

2.6.3. Intra-particle diffusion

This model is generally used for adsorption mechanism identification for design purpose [45]. For most adsorption process, the uptake varies proportionally with $t^{\,o}$ rather than with contact time as represented by the following equation [38].

$$q_t = K_{id}t^{0.5} \tag{9}$$

where K_{id}(mg/g.$min^{0.5}$) is the rate constant of intra-particle diffusion, and $t^{\,0.5}$ (min) is the square root of time. Plotting $q_t$vs $t^{\,0.5}$ gives a linear relationship. Then K_{id} value can be decided from the slope of the plot.

2.6.4. Liquid film diffusion

In liquid and solid adsorption system, the rate of accumulated solute in the solid phase is equal to that of solute transfer and can be written as follows [38,46].

$$ln\left(1 - \frac{q_t}{q_e}\right) = -K_{fd}t \tag{10}$$

where $ln\left(1 - \frac{q_t}{q_e}\right)$ is the fractional attainment of equilibrium, and K_{fd} is the film diffusion rate constant. By plotting $ln\left(1 - \frac{q_t}{q_e}\right)$ vs t, it gives a linear relationship, then K_{fd}can be obtained from the slope of the plot.

2.6.5. Double-exponential

A double exponential function model can be written as follows [47].

$$q_t - q_e = exp(-k_1 t) - exp(-k_2 t) \tag{11}$$

If $k_1 \gg k_2$, it means that the rapid process can be assumed to be negligible on the overall kinetics, and the linearized form of the equation can be written as follows:

$$ln(q_e - q_t) = -k_2 t \tag{12}$$

where K_1 (min^{-1}) is diffusion parameter of the rapid step, and K_2 is for the slow step. Plotting ln (q_e-q_t) vs t gives a linear relationship, and K_2 can be obtained from the slope of the plot.

2.7. Thermodynamics analysis

The thermodynamics parameters, such as changes in Gibb's free energy (ΔG^o), enthalpy (ΔH^o), and entropy (ΔS^o), have been determined in order to understand the reaction changes during the process using the following Eqs. (13) and (14) [32]. In this case, COD removal efficiency values under varying temperatures were used.

$$\Delta G^0 = \Delta H^0 - T\Delta S^0 \tag{13}$$

$$log\left(\frac{q_e}{C_e}\right) = \frac{\Delta S^o}{2.303R} + \frac{-\Delta H^o}{2.303RT} \tag{14}$$

where q_e is the solid-phase concentration at equilibrium (mg/L), and C_e is equilibrium concentration in solution (mg/L). The values of ΔS^o and ΔH^0 can be calculated from the intercept and slope of the linear Van't Hoff plot log $\left(\frac{q_e}{C_e}\right)$ vs. $1/T$. From those values, then Gibb's free energy (ΔG^0) can be determined.

3. Results and discussion

3.1. Biosorbent characterization

3.1.1. Surface chemistry and elemental analysis

Some important surface chemistry characteristics of eucalyptus bark in its raw version such as specific surface area, total pore volume, and average pore size were measured while the elemental analysis of the biosorbent was also evaluated using elemental analyzer. Then the results are presented in Table 2.

Based on the table, it can be seen that REB has sufficient surface area and bulk density in which they are valuable matters for the sorbent to act as capable biosorbent since the advised decent value of bulk density for practical adsorption process should be higher than 0.25 g/cm^{-3} [32]. While specific surface area was accounted using BET equation, total pore volume was calculated by converting the adsorption volume of nitrogen at relative pressure 0.95 to equivalent adsorbate liquid volume [48]. In accordance with elemental assessment, the vast majority element of REB is carbon by 40.39%, followed by oxygen as the second highest component. Hydrogen and nitrogen, at the same time, sit as other elements detected in less significant amount. Nevertheless, this is common in plant-based adsorbent materials including EB as due to its organic content [32,39].

Table 2 Physico-chemical properties of REB.

Parameters	Values
BET surface area (m^2/g)	6.1178
Bulk density (gm/cm^{-3})	0.37
Total pore volume (cm^3/g)	0.00355
Average pore size (A°)	18.42
Nitrogen, N (%)	0.24
Carbon, C (%)	40.39
Hydrogen, H (%)	5.49
Oxygen, O (%)	35.5

3.1.2. FTIR analysis

Fig. 2a–c describe FTIR images which were used to analyze the functional groups of REB and both of hybrid MEB before and after pollutants removal process.

For REB (Fig. 2a), several peaks were observed such as at 3339.2, 2923.5, and 1730.6 cm^{-1} that can be assigned to N–H, C–H, and C = O cm^{-1} stretching, respectively [49]. Peak at 1615.7 cm^{-1} is due to C = O bend with nitro groups while the strong asymmetric stretching N–O and medium C–C bond in aromatics were shown at 1518.6 and 1443.9 cm^{-1}, respectively. The existence of alcohols, esters, and ethers functional groups was detected through C–O strong stretch in the adsorption band of 1320 – 1000 cm^{-1} frequency range with some absorption peaks at 1317.5, 1236, and 1032 cm^{-1}, respectively [50,51]. Peak at 780 cm^{-1} confirmed the = C–H bend with alkene group [51].

For hybrid MEB before pollutant removal (Fig. 2b), the spectrums show some heteroatoms bonding to the edges of the carbon layers which govern the surface chemistry of sorbent. Broad band at 1000–1300 cm^{-1} (maxima at 1190–1200 cm^{-1}) can be considered as a characteristic of phosphorous and phosphor carbonaceous compounds present in the phosphoric acid activated carbons [52,53], while peak at 1607.9 cm^{-} can be assigned to C–C = C asymmetric stretch with alkenes functional groups [50]. Afterwards, Fig. 2c representing the spectrums of hybrid MEB after pollutant removal process displays some new peaks such as 3329.7, 2853.2, and 1745.2 cm^{-1} indicating the existence of phenol, alkanes, and ketone functional groups, respectively [50].

3.1.3. Spectrometric surface morphological analysis

To examine the morphology of REB biomass, scanning electron micrograph (SEM) was applied, and the image shown in Fig. 3 indicated that naturally raw EB has adequate pores that are amorphous carbon with non-crystalline structure. This pore structure is required as a place for adsorbed pollutant trapped in the internal surface of the sorbent.

3.2. Effect of modification process

The initial modification positively affects the efficacy of EB to adsorb targeted pollutants in the effluent. To assess how modification methods influencing on the performance of EB, the comparison of selected pollutants removal efficiency amongst REB, chemically treated EB using different chemical solutions ($ZnCl_2$, NaOH, and H_3PO_4), carbonized EB, and MEB by hybrid treatment was studied. The biosorbent which was previously treated using decided chemical solution was examined regarding its performance for COD, oil, and Cr(III) removals in raw PRE using 10 g/L of biosorbent dosage for 100 min of contact time. According to Fig. 4, it can be noticed that H_3PO_4 figured better values of COD, oil, and Cr(III) removal efficiencies by more than 55, 66, and 41%, respectively. This result is similar to several studies reporting that H_3PO_4 is a reliable effective dehydrating agent as it can promote higher dehydration, better pyrolytic decomposition, and more cross-linked structure establishment [54,55]. This conditions support pores generation expanding biomass structure that is fundamental for adsorption capacity because it can increase fibrous structure of raw organic materials and enlarge them [6]. Additionally, acidic atmosphere also attributes to functional surface

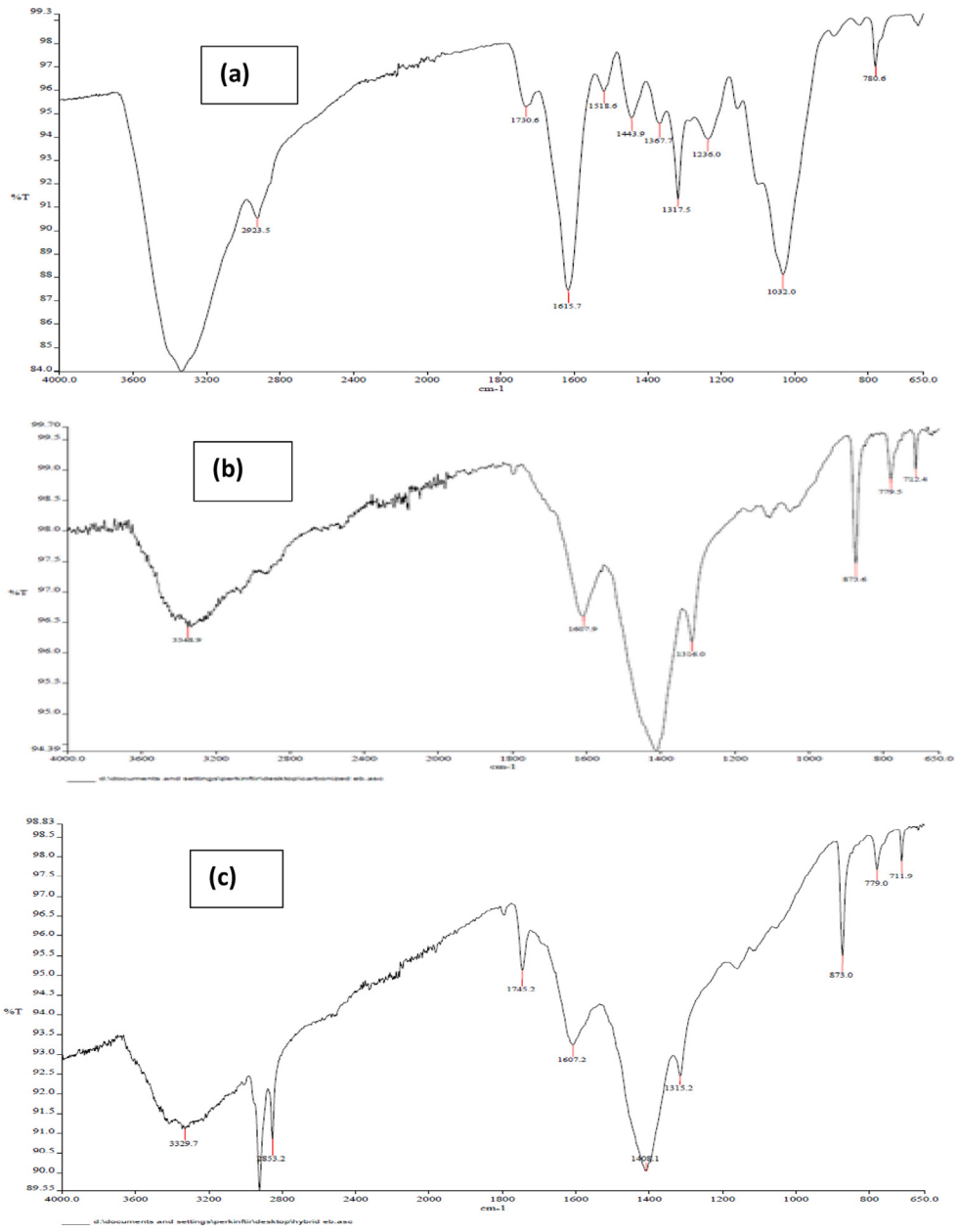

Fig. 2 FTIR spectrum (a) REB (b) Hybrid H_3PO_4 + Carbonization MEB before pollutant removal (c) Hybrid H_3PO_4 + Carbonization MEB after pollutant removal.

group dissociation resulting in an increase in charge densities [28,56].

Fig. 5 shows further preliminary tests for varying biosorbent modification assessment. As H_3PO_4 performed better on targeted pollutant removal, it was then compared to other MEB; namely carbonized and hybrid MEB. From this point, biosorbent treated by hybrid treatment performed tangibly better achievement for COD, oil, and Cr(III) removal values by more than 72, 88, and 54%, respectively. Based on the figure, it is also worthy to mention that despite having less targeted pollutant reduction than chemical modified EB, stand-alone carbonized EB has comparatively effective results as during carbonization process, the biosorbent is pyrolyzed to eliminate low molecular weight and volatiles organic residues creating higher carbon content material and more mesoporous structure [57,58]. Since hybrid MEB sorbent showed better removal efficiency, it ultimately was chosen to be applied for further experiments to assess the effect of different operating conditions on COD, oil, and Cr(III) removal efficiency.

3.3. Adsorption studies

3.3.1. Effect of contact time

The effect of varying contact time between hybrid MEB and raw PRE on the removal efficiencies of COD, oil, and Cr (III) was investigated under constant operating conditions of pH 3, temperature 30 °C, agitation speed 200 rpm, and sorbent

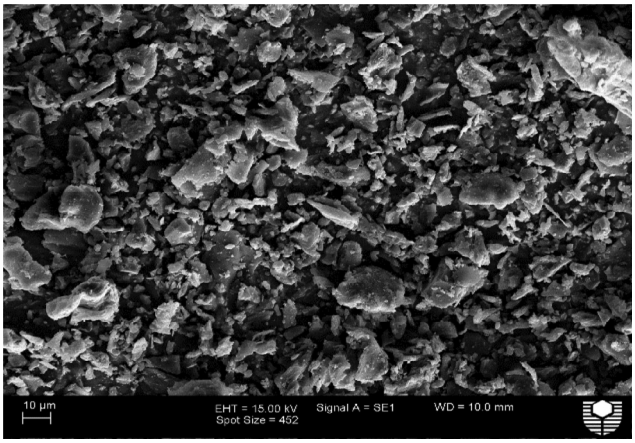

Fig. 3 SEM analysis of raw EB biosorbent.

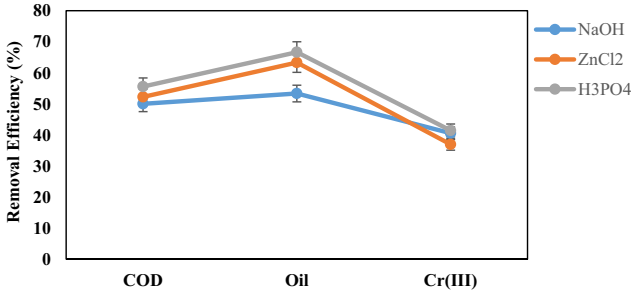

Fig. 4 Removal efficiency of COD, oil, and Cr(III) in raw PRE using chemically treated EB.

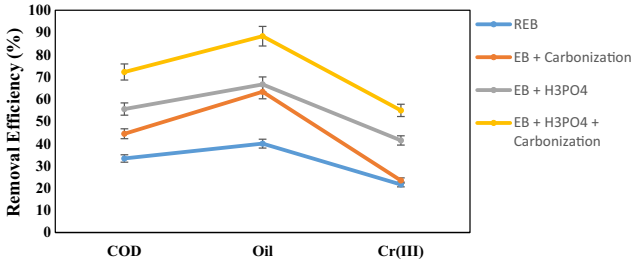

Fig. 5 The comparison of COD, oil, and Cr(III) removal efficiencies from raw PRE using raw and modified EB.

dosage 10 g/L. Based on the experimental results shown in Fig. 6, contact time has a tangible effect on the removal efficiency of the targeted pollutants. As can also be seen in the figure, all removal efficiencies increased with the increase in contact time. Longer immersion time of sorbent in the effluent can increase the amounts of metal ions, oil particles, and COD pollutants adsorbed onto sorbent material [23,59]. The adsorption rate increased fast in the first 70 min for both COD and Cr (III) and in the first 100 min for oil adsorption. This is caused by the large availability of free binding sorbent sites at certain initial contact time creating more attraction between pollutant particles and sorbent to interact with each other [15,45,60]. However, it was observed that the removal process reached the equilibrium point at 100 min for all three types of pollutants. At that point, the removal efficiency tended to level

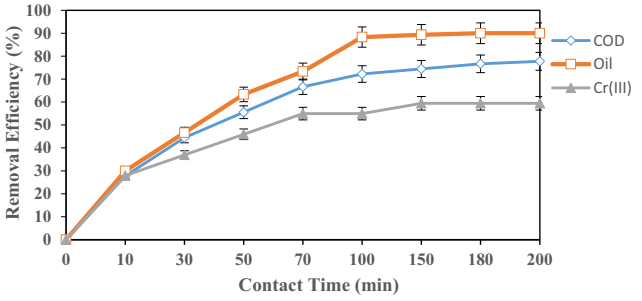

Fig. 6 Effect of contact time (sorbent dosage; 10 g/L, pH; 3, T; 25 °C, Agitation speed; 200 rpm).

off due to limited surface available for pollutant particles capture [18,61]. Thus this study found that, at 200 min, the maximum removal efficiencies achieved were 77, 90, and 59% for COD, oil, and Cr(III), respectively.

3.3.2. Effect of pH

The effect of initial pH on pollutants removal efficiency was also investigated at different pH values (3, 5, 7, 9, and 10) while other operating conditions were still kept constant. As can be observed in Fig. 7, pH has a prominent role to the fluctuation of oil and Cr(III) removal profiles where the maximum removal occurred at acidic pH of 3. For metal adsorption, pH is one of the important parameters as it can control the protonation of the functional groups on the sorbent materials [62]. Mostly, metal ions removal is favorable in acidic atmosphere even though certain metals reported showing increasing removal percentage at higher alkaline solution [6,63].

For oil removal section, the influence of acidic pH environment can promote oil droplets to destabilize by supporting de-emulsification and larger oil droplets formation which enhanced oil adsorption onto the hybrid MEB sorbent surface. Conversely, at alkaline pH, the saponification process occurred dominantly which caused lower oil content removal [15]. At neutral pH, oil removal efficiency is lower than that of in both acidic and alkaline solutions which can be correlated to the destabilization of organic sorbent materials at neutral pH environment [64]. Furthermore, compared to oil and Cr (III) profiles, the effect of solution pH on COD removal tends to have insignificant influence on the adsorption process as there were slight enhancement of COD removal for all pH values ranging from 3 to 10. In addition, several studies reported nearly similar results regarding pH function on COD adsorption using different organic sorbent materials [4,65].

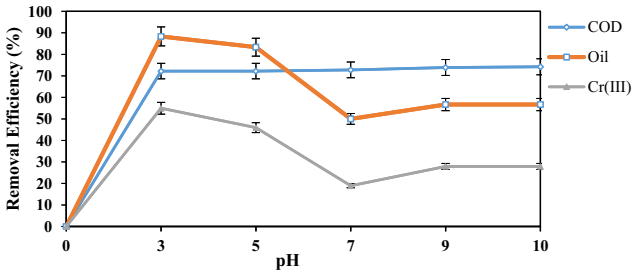

Fig. 7 Effect of pH (T; 25 °C, sorbent dosage; 10 g/L, t; 100 min, agitation speed; 200 rpm).

3.3.3. Effect of temperature

Effect of temperature was measured at varying values. Based on the observation of experimental results depicted in Fig. 8, temperature has to be considered as part of notable aspects in targeted pollutants removal, especially for oil and Cr(III) adsorption processes.

It can be witnessed that, at lower temperatures (25 – 30 °C), both oil and Cr(III) reached better removal efficiency by more than 88 and 54%, respectively. Then they gradually decreased at higher temperatures. For oil removal, this lowering trend can be caused by several factors including lower viscosity of raw PRE solution resulting monolayer oil adsorption on sorbent surface at higher solution temperature, increasing Brownian motion of oil molecules that decreasing their entrapment onto sorbent surface and higher energy needed to attach oil particles [18,66]. For Cr(III) decrease with increasing temperature, this demonstrates that the adsorption of metal ions onto sorbent material is exothermic in nature [67,68]. Reversely, better performance of sorbent to adsorb oil at lower temperature might be supported by more interaction between oil and sorbent during adsorption process due to the effect of higher diffusion rate of the adsorbate molecules across sorbent surface [20,64]. In accordance with COD profile, for an increase in temperature, there is an insignificant change which may be attributed to the increase in the kinetic energy of the adsorbate with temperature enhancing the adsorbate availability at the active sites of the MEB sorbent. Therewith increasing temperature can slightly booster the pore expansion within the sorbent particles escalating the COD pollutants adsorption capacity [4].

3.3.4. Effect of dosage

In order to study the effect of sorbent dosage on the profile of targeted pollutants removal, the experiments were conducted by applying assorted dosage values (5, 10, 15, 20, and 25 g/L) in the effluent. Fig. 9 shows that the increasing the dosage increased the removal efficiency of three types of pollutants up to 80, 90, and 61% for COD, oil and Cr(III), respectively, at maximum dosage of 25 g/L. This figure also envisages that the more sorbent dosage used to absorb the adsorbate particles, the higher the availability of the active sites for sorbent potential binding [15,69]. As shown in Fig. 9, COD, oil, and Cr(III) removal efficiencies gradually increased from 55 to 72%, from 66 to 88%, and from 36 to 54%, respectively, with the rise in hybrid MEB dosage from 5 to 10 g/L. However, the figure also confirms that increasing sorbent dosage beyond 10 g/L had less effect on oil and Cr(III) reduction,

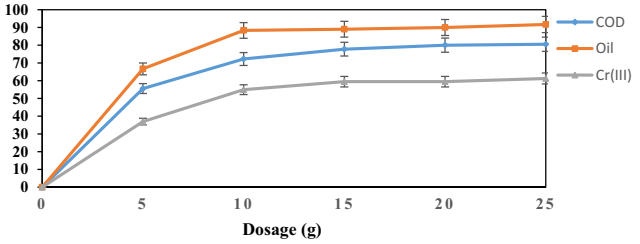

Fig. 9 Effect of biosorbent dosage (T; 25 C, pH; 3, t; 100 min, agitation speed; 200 rpm).

and hence this value was considered as the optimum dosage while for COD removal, the optimum sorbent dosage observed was 15 g/L. In addition, the uptake which decreases with increasing the amount of dosage can be attributed to several factors such as the availability of solute, limited amount of adsorbate that can be adsorbed by sorbent surface, interference between binding sites, electrostatic interactions, and less mixing chance due to high adsorbent concentration in the solution [4,44,70].

3.3.5. Sorbent regeneration

Hybrid MEB regeneration was also examined in order to study its reusability efficiency by rinsing method using pure water and varying salt solutions; namely $NaHCO_3$, NH_4HSO_4, and NaCL. As oil adsorption rate consistently showed better removal percentage in previous experiments under varying operating conditions, this parameter was therefore used in the sorbent regeneration analysis. The results shown in Fig. 10 propose the use of rinsing technique to repair the effectiveness of saturated hybrid MEB for oil adsorption. Based on the figure, we can notice that both water and salt solutions can partly remove the adsorbed oil from previous cycle.

However, this regeneration has limited efficacy since rinsing method showed its significant performance only up to the fourth adsorption cycle with 50 to 60% of oil were removed from raw PRE. Then it consistently alleviated at the further cycle. Other than that, it was also observed that alkaline solution represented by $NaHCO_3$ can act better in removing and washing away organic pollutants including trapped oils content on sorbent surface via hydrolysis and solubilisation reactions [71]. This results indicated that hybrid MEB has an adequate regeneration ability that plays a vital role as a sorbent material.

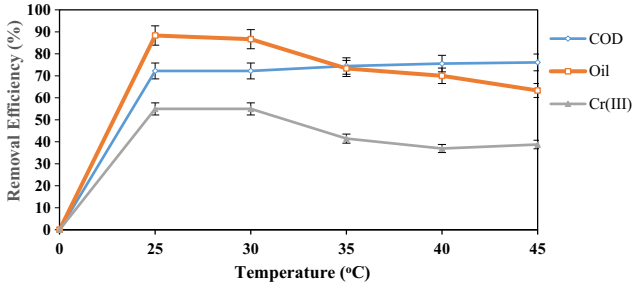

Fig. 8 Effect of temperature (sorbent dosage; 10 g/L, pH; 3, t; 100 min, agitation speed; 200 rpm).

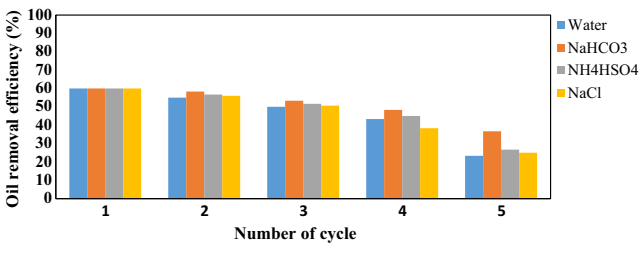

Fig. 10 The regeneration of hybrid MEB using different rinsing solutions.

3.3.6. Adsorption isotherm

To understand the interactive nature between the adsorbate and hybrid MEB sorbent and design the efficient adsorption system, the equilibrium adsorption isotherm analysis can be implemented. This study applied three isotherm fitting models; namely Langmuir, Freundlich, and Dubinin–Radushkevich isotherm models for Cr(III) ions adsorption taken as an example case (Figs. 11–13). It found that Freundlich isotherm model has best fitting with the R^2 value which tends to be much closer to 1 (Table 3).

Freundlich model was analyzed by fitting adsorption equilibrium data with experimental data (Fig. 12) where the value of correlation coefficient obtained is 0.9758. The values of K_f and N were calculated from the slope and intercept of the plot between lnq_e vs. lnC_e. This model assumes that the adsorption process takes place on heterogeneous surface, and the amount of adsorbate adsorbed per unit weight of sorbent is related to the concentration of adsorbed Cr(III) ions at equilibrium.

3.3.7. Adsorption kinetic modelling

The experimental data was fitted using pseudo-first order, pseudo-second order, intra-particle diffusion, liquid film diffusion, and double exponential models in accordance with the kinetic analysis of Cr(III) ions onto hybrid MEB sorbent. The experiments were conducted under operating conditions of pH 3, temperature 25 °C, agitation speed 200 rpm, and sorbent dosage 10 g/L. As can be seen in Table 4, the equilibrium adsorption of intra-particle diffusion model which is confirmed by performing the regression analysis on experimental data seemed to be the best one compared with the other kinetic models. According to intra-particle diffusion model, if a plot of adsorption capacity, q_t, vs. square foot of contact time illustrates a linear plot, it predicts that intra-particle/pore diffusion is the rate-limiting step during the adsorption process [32,44]. Therefore, the adsorption of Cr(III) from raw PRE onto hybrid MEB sorbent is considered more as an intra-particle diffusion model reaction with the R^2 value of 0.9822, but it also suggested that some other mechanism might be involved.

3.3.8. Thermodynamic analysis

Thermodynamic study has been investigated based on the equilibrium data, and all the calculated thermodynamic parameters are presented in Table 5. From the table, the change in Gibbs free energy(ΔG^0) was found to be positive at all temperatures indicating that nature of the process is unfavourable or non-spontaneous. Enthalpy (ΔH^0) positive value means that during adsorption process, the reactions occurred in endothermic mode while the positive value of entropy (ΔS^0) indicates favourable randomness factor though

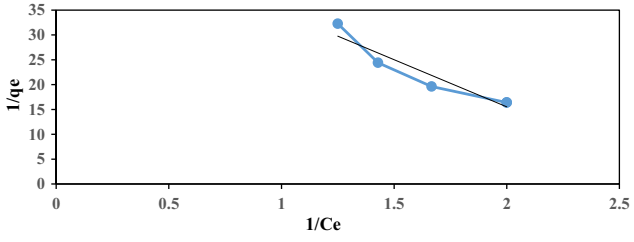

Fig. 11 Langmuir isoterm model for Cr(III) adsorption.

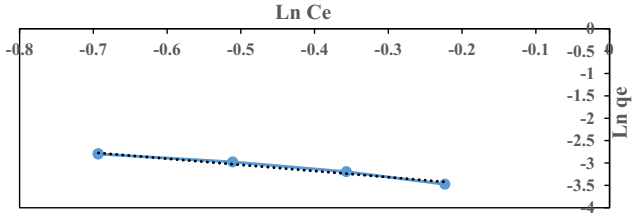

Fig. 12 Freundlich isoterm model for Cr(III) adsorption.

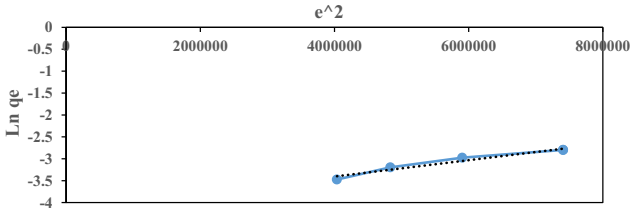

Fig. 13 Dubinin–Radushkevich isoterm model for Cr(III) adsorption.

Table 3 Parameters of Langmuir, Freundlich, and Dubinin-Radushkevich isotherm models for Cr(III) adsorption.

Langmuir	Values
K_L (L/mg)	0.00628
q_m(mg/g)	0.0263
R^2	0.9069
Freudlich	
K_f	3.7337
N	−1.3704
R^2	0.9758
Dubinin-Radushkevich	
q_m(mg/g)	0.033
β	0.0074
R^2	0.9528

Table 4 Adsorption kinetic model parameters.

Pseudo-first order model	Values
$q_{e\ experimental\ (mg/g)}$	0.066
$q_{e\ calculated\ (mg/g)}$	0.061433499
K_1 (min^{-1})	0.0764596
R^2	0.943
Pseudo-second order model	
$q_{e\ calculated\ (mg/g)}$	7.342143906
K_2 (mg/gmin)	0.00340375
R^2	0.9613
h (mg/gmin)	0.183486239
Intra-particle diffusion model	
K_{id} (min^{-1})	0.5708
R^2	0.9822
Liquid film diffusion model	
K_{fd}(min^{-1})	0.0317
R^2	0.9291
Double exponential model	
K_2 (min^{-1})	0.0317
R^2	0.9291

Table 5 Thermodynamic parameters at different temperature.

Temp. (K)	ΔG° (KJ/mole)	ΔH° (KJ/mole)	ΔS° (KJ/mole K)
298.15	3.39		
303.15	3.29		
308.15	3.19	9.13	0.02
313.15	3.10		
318.15	3.00		

its value is small [72]. Accordingly, this suggests the structural changes after adsorption takes place on the sorbent.

4. Conclusions

This work showed that PRE can be treated using EB sorbent in terms of its COD, oil, and Cr(III) contents removal. Compared to raw and modified EB using chemical activation and carbonization, EB which has been previously activated by hybrid chemical treatment and carbonization process was found to have better pollutants removal efficiency. Experimental results showed that increasing dosage and contact time increased the removal efficiency of all three types of pollutants until certain values. While acidic pH and lower temperature were found as the most favorable conditions for both oil and Cr(III) removal, they seemed to have less significant effect on COD adsorption change. Furthermore, adsorption isotherm that was analyzed using Langmuir, Freundlich, and Dubinin-Radushkevich isotherm models found Freundlich model as the best fitted model (R^2 value of 0.9758). Kinetic analysis proved that the adsorption kinetic follows the intraparticle diffusion model (R^2 value of 0.9822). Additionally, thermodynamic study showed that the adsorption process occurred in non-spontaneous and endothermic reactions. This hybrid MEB has also a reliable regeneration ability by simple washing methods for about four time cycles using alkaline solution. Overall, this study demonstrates that modified EB using H_3PO_4/carbonization can be the alternative for many expensive commercial adsorbents used for the removal of pollutant contents such as COD, oil, and Cr(III) ions from actual industrial oily wastewaters including petroleum refinery effluent.

Declaration of Competing Interest

The author declare that there is no conflict of interest.

References

[1] S. Varjani, R. Joshi, V.K. Srivastava, H.H. Ngo, W. Guo, Treatment of wastewater from petroleum industry: current practices and perspectives, Environ. Sci. Pollut. Res. (2019) 1–9.

[2] S. Martini, H.M. Ang, Hybrid TiO_2/UV/PVDF ultrafiltration membrane for raw canola oil wastewater treatment, Desalination Water Treat. 148 (2019) 51–59.

[3] A. Bhatnagar, M. Sillanpää, A. Witek-Krowiak, Agricultural waste peels as versatile biomass for water purification – a review, Chem. Eng. J. 270 (2015) 244–271.

[4] M.H. El-Naas, S. Al-Zuhair, M.A. Alhaija, Reduction of COD in refinery wastewater through adsorption on date-pit activated carbon, J. Hazard. Mater. 173 (2010) 750–757.

[5] D. Angelova, I. Uzunov, S. Uzunova, A. Gigova, L. Minchev, Kinetics of oil and oil products adsorption by carbonized rice husks, Chem. Eng. J. 172 (2011) 306–311.

[6] M. Danish, T. Ahmad, A review on utilization of wood biomass as a sustainable precursor for activated carbon production and application, Renew. Sustain. Energy Rev. 87 (2018) 1–21.

[7] G.F. Coelho, A.C. Gonçalves Jr, C.R.T. Tarley, J. Casarin, H. Nacke, M.A. Francziskowski, Removal of metal ions Cd (II), Pb (II), and Cr (III) from water by the cashew nut shell Anacardium occidentale L, Ecol. Eng. 73 (2014) 514–525.

[8] S. Martini, H.M. Ang, H. Znad, Integrated ultrafiltration membrane unit for efficient petroleum refinery effluent treatment, CLEAN – Soil Air Water 45 (2017) 1600342.

[9] A. Coelho, A.V. Castro, M. Dezotti, G.L. Sant'Anna, Treatment of petroleum refinery sourwater by advanced oxidation processes, J. Hazard. Mater. 137 (2006) 178–184.

[10] L. Yan, H. Ma, B. Wang, W. Mao, Y. Chen, Advanced purification of petroleum refinery wastewater by catalytic vacuum distillation, J. Hazard. Mater. 178 (2010) 1120–1124.

[11] D. Aljubourya, P. Palaniandy, H. Aziz, S. Feroz, Comparative study to the solar photo-fenton, solar photocatalyst of TiO_2 and solar photocatalyst of TiO_2 combined with fenton process to treat petroleum wastewater by RSM, J. Petrol. Environ. Biotechnol. 2016 (2016).

[12] L. Cai, Y. Zhang, Y. Zhou, X. Zhang, L. Ji, W. Song, H. Zhang, J. Liu, Effective adsorption of diesel oil by crab-shell-derived biochar nanomaterials, Materials (Basel) 12 (2019) 236.

[13] W. Chai, X. Liu, J. Zou, X. Zhang, B. Li, T. Yin, Pomelo peel modified with acetic anhydride and styrene as new sorbents for removal of oil pollution, Carbohydr. Polym. 132 (2015) 245–251.

[14] S. Ibrahim, H.-M. Ang, S. Wang, Removal of emulsified food and mineral oils from wastewater using surfactant modified barley straw, Bioresour. Technol. 100 (2009) 5744–5749.

[15] A.L. Ahmad, S. Sumathi, B.H. Hameed, Adsorption of residue oil from palm oil mill effluent using powder and flake chitosan: equilibrium and kinetic studies, Water Res. 39 (2005) 2483–2494.

[16] B. Doshi, M. Sillanpää, S. Kalliola, A review of bio-based materials for oil spill treatment, Water Res. 135 (2018) 262–277.

[17] D. Peng, Z. Lan, C. Guo, C. Yang, Z. Dang, Application of cellulase for the modification of corn stalk: Leading to oil sorption, Bioresour. Technol. 137 (2013) 414–418.

[18] R. Wahi, L.A. Chuah, Z. Ngaini, M.M. Nourouzi, T.S.Y. Choong, Esterification of M. sagu bark as an adsorbent for removal of emulsified oil, J. Environ. Chem. Eng. 2 (2014) 324–331.

[19] M. Abdullah, S.H.A. Muhamad, S.N. Sanusi, S.I.S. Jamaludin, N.F. Mohamad, M.A.H. Rusli, Preliminary study of oil removal using hybrid peel waste: musa balbisiana and citrus sinensis, J. Appl. Environ. Biol. Sci. 6 (2016) 59–63.

[20] S. Ibrahim, S. Wang, H.M. Ang, Removal of emulsified oil from oily wastewater using agricultural waste barley straw, Biochem. Eng. J. 49 (2010) 78–83.

[21] S. Suni, A.L. Kosunen, M. Hautala, A. Pasila, M. Romantschuk, Use of a by-product of peat excavation, cotton grass fibre, as a sorbent for oil-spills, Mar. Pollut. Bull. 49 (2004) 916–921.

[22] V. Nejadshafiee, M.R. Islami, Adsorption capacity of heavy metal ions using sultone-modified magnetic activated carbon as a bio-adsorbent, Mater. Sci. Eng., C 101 (2019) 42–52.

[23] S.A. Sadeek, N.A. Negm, H.H. Hefni, M.M.A. Wahab, Metal adsorption by agricultural biosorbents: adsorption isotherm, kinetic and biosorbents chemical structures, Int. J. Biol. Macromol. 81 (2015) 400–409.

[24] M. Basu, A.K. Guha, L. Ray, Adsorption of lead on lentil husk in fixed bed column bioreactor, Bioresour. Technol. 283 (2019) 86–95.

[25] R. Wahi, L.C. Abdullah, M.N. Mobarekeh, Z. Ngaini, T.C.S. Yaw, Utilization of esterified sago bark fibre waste for removal of oil from palm oil mill effluent, J. Environ. Chem. Eng. 5 (2017) 170–177.
[26] S.S. Banerjee, M.V. Joshi, R.V. Jayaram, Treatment of oil spill by sorption technique using fatty acid grafted sawdust, Chemosphere 64 (2006) 1026–1031.
[27] A. Ghaedi, M. Ghaedi, A. Vafaei, N. Iravani, M. Keshavarz, M. Rad, I. Tyagi, S. Agarwal, V.K. Gupta, Adsorption of copper (II) using modified activated carbon prepared from Pomegranate wood: optimization by bee algorithm and response surface methodology, J. Mol. Liq. 206 (2015) 195–206.
[28] R.S. Souza, P.S.S. Porto, A.M.A. Pintor, G. Ruphuy, M.F. Costa, R.A.R. Boaventura, V.J.P. Vilar, New insights on the removal of mineral oil from oil-in-water emulsions using cork by-products: Effect of salt and surfactants content, Chem. Eng. J. 285 (2016) 709–717.
[29] L.C. Morais, O.M. Freitas, E.P. Gonçalves, L.T. Vasconcelos, C.G. González Beça, Reactive dyes removal from wastewaters by adsorption on eucalyptus bark: variables that define the process, Water Res. 33 (1999) 979–988.
[30] I. Ghodbane, L. Nouri, O. Hamdaoui, M. Chiha, Kinetic and equilibrium study for the sorption of cadmium(II) ions from aqueous phase by eucalyptus bark, J. Hazard. Mater. 152 (2008) 148–158.
[31] V. Sarin, K.K. Pant, Removal of chromium from industrial waste by using eucalyptus bark, Bioresour. Technol. 97 (2006) 15–20.
[32] S. Afroze, T.K. Sen, M. Ang, H. Nishioka, Adsorption of methylene blue dye from aqueous solution by novel biomass Eucalyptus sheathiana bark: equilibrium, kinetics, thermodynamics and mechanism, Desalin. Water Treat. (2015) 1–21.
[33] S. Afroze, T.K. Sen, H.M. Ang, Adsorption removal of zinc (II) from aqueous phase by raw and base modified Eucalyptus sheathiana bark: Kinetics, mechanism and equilibrium study, Process Saf. Environ. Prot. 102 (2016) 336–352.
[34] P. Patnukao, P. Pavasant, Activated carbon from Eucalyptus camaldulensis Dehn bark using phosphoric acid activation, Bioresour. Technol. 99 (2008) 8540–8543.
[35] S. Dawood, T.K. Sen, C. Phan, Adsorption removal of Methylene Blue (MB) dye from aqueous solution by bio-char prepared from Eucalyptus sheathiana bark: kinetic, equilibrium, mechanism, thermodynamic and process design, Desalin. Water Treat. 57 (2016) 28964–28980.
[36] S. Zulaikha, W.J. Lau, A.F. Ismail, J. Jaafar, Treatment of restaurant wastewater using ultrafiltration and nanofiltration membranes, J. Water Process Eng. 2 (2014) 58–62.
[37] I. Morosanu, C. Teodosiu, C. Paduraru, D. Ibanescu, L. Tofan, Biosorption of lead ions from aqueous effluents by rapeseed biomass, New Biotechnol. 39 (2017) 110–124.
[38] M.A. Ahsan, S.K. Katla, M.T. Islam, J.A. Hernandez-Viezcas, L.M. Martinez, C.A. Díaz-Moreno, J. Lopez, S.R. Singamaneni, J. Banuelos, J. Gardea-Torresdey, Adsorptive removal of methylene blue, tetracycline and Cr (VI) from water using sulfonated tea waste, Environ. Technol. Innovation 11 (2018) 23–40.
[39] S. Dawood, T. Sen, C. Phan, Synthesis and characterisation of novel-activated carbon from waste biomass pine cone and its application in the removal of congo red dye from aqueous solution by adsorption, Water Air Soil Pollut 225 (2013) 1–16.
[40] M. Dubinin, L. Radushkevich, Evaluation of microporous material with a new isotherm, Dokl Akad Nauk SSSR (1966) 331–347.
[41] S.Y. Lagergren, Zur Theorie der sogenannten Adsorption gelöster, Stoffe (1898).
[42] B.K. Nandi, A. Goswami, M.K. Purkait, Removal of cationic dyes from aqueous solutions by kaolin: kinetic and equilibrium studies, Appl. Clay Sci. 42 (2009) 583–590.
[43] T.K. Sen, M.V. Sarzali, Removal of cadmium metal ion (Cd2 +) from its aqueous solution by aluminium oxide (Al_2O_3): a kinetic and equilibrium study, Chem. Eng. J. 142 (2008) 256–262.
[44] A. El Shahawy, G. Heikal, Organic pollutants removal from oily wastewater using clean technology economically, friendly biosorbent (Phragmites australis), Ecol. Eng. 122 (2018) 207–218.
[45] T. Sen, S. Afroze, H.M. Ang, Equilibrium, kinetics and mechanism of removal of methylene blue from aqueous solution by adsorption onto pine cone biomass of Pinus radiata, Water Air Soil Pollut 218 (2011) 499–515.
[46] G.E. Boyd, A.W. Adamson, L.S. Myers, The exchange adsorption of ions from aqueous solutions by organic zeolites. 11 Kinetics, J. Am. Chem. Soc. 69 (1947) 2836–2848.
[47] A. Wilczak, T.M. Keinath, Kinetics of sorption and desorption of copper(II) and lead (II) on activated carbon, Water Environ. Res. 65 (1993) 238–244.
[48] J. De Boer, B. Linsen, T. Van der Plas, G. Zondervan, Studies on pore systems in catalysts: VII Description of the pore dimensions of carbon blacks by the t method, J. Catal. 4 (1965) 649–653.
[49] T.o.C.I. Absorptions, Table of Characteristic IR Absorptions, in, University of Colorado, 1985.
[50] T.P.I.A.f.C.F. Groups, Table 1: Principal IR Absorptions for Certain Functional Groups in, Wellesley College, 1875.
[51] T.o.C.I. Absorption, Tables of Characteristic IR Absorption, in, University of Colorado, 1985.
[52] A. Puziy, O. Poddubnaya, A. Martınez-Alonso, F. Suárez-Garcıa, J. Tascón, Synthetic carbons activated with phosphoric acid: I. Surface chemistry and ion binding properties, Carbon 40 (2002) 1493–1505.
[53] S. Yakout, G.S. El-Deen, Characterization of activated carbon prepared by phosphoric acid activation of olive stones, Arab. J. Chem. 9 (2016) S1155–S1162.
[54] S. Yorgun, D. Yıldız, Preparation and characterization of activated carbons from Paulownia wood by chemical activation with H3PO4, J. Taiwan Inst. Chem. Eng. 53 (2015) 122–131.
[55] A. Heidari, H. Younesi, A. Rashidi, A. Ghoreyshi, Adsorptive removal of CO2 on highly microporous activated carbons prepared from Eucalyptus camaldulensis wood: Effect of chemical activation, J. Taiwan Inst. Chem. Eng. 45 (2014) 579–588.
[56] M. Daaou, D. Bendedouch, Water pH and surfactant addition effects on the stability of an Algerian crude oil emulsion, J. Saudi Chem. Soc. 16 (2012) 333–337.
[57] L. Daza, S. Mendioroz, J. Pajares, Preparation of Rh/active carbon catalysts by adsorption in organic media, Carbon 24 (1986) 33–41.
[58] J. González, S. Román, J.M. Encinar, G. Martínez, Pyrolysis of various biomass residues and char utilization for the production of activated carbons, J. Anal. Appl. Pyrol. 85 (2009) 134–141.
[59] W. Pitakpoolsil, M. Hunsom, Adsorption of pollutants from biodiesel wastewater using chitosan flakes, J. Taiwan Inst. Chem. Eng. 44 (2013) 963–971.
[60] A. Dąbrowski, Adsorption—from theory to practice, Adv. Colloid Interface Sci. 93 (2001) 135–224.
[61] A. Srinivasan, T. Viraraghavan, Removal of oil by walnut shell media, Bioresour. Technol. 99 (2008) 8217–8220.
[62] N. Feng, X. Guo, S. Liang, Y. Zhu, J. Liu, Biosorption of heavy metals from aqueous solutions by chemically modified orange peel, J. Hazard. Mater. 185 (2011) 49–54.
[63] K. Banerjee, S. Ramesh, R. Gandhimathi, P. Nidheesh, K. Bharathi, A novel agricultural waste adsorbent, watermelon shell for the removal of copper from aqueous solutions, Iran, J. Energy Environ. 3 (2012) 143–156.

[64] V. Rajaković-Ognjanović, G. Aleksić, L. Rajaković, Governing factors for motor oil removal from water with different sorption materials, J. Hazard. Mater. 154 (2008) 558–563.
[65] A.K. Parande, A. Sivashanmugam, H. Beulah, N. Palaniswamy, Performance evaluation of low cost adsorbents in reduction of COD in sugar industrial effluent, J. Hazard. Mater. 168 (2009) 800–805.
[66] G. Alaa El-Din, A.A. Amer, G. Malsh, M. Hussein, Study on the use of banana peels for oil spill removal, Alexandria Eng. J. 57 (2018) 2061–2068.
[67] S. Abedi, H. Zavvar Mousavi, A. Asghari, Investigation of heavy metal ions adsorption by magnetically modified aloe vera leaves ash based on equilibrium, kinetic and thermodynamic studies, Desalin. Water Treat. 57 (2016) 13747–13759.
[68] A.G. Adeniyi, J.O. Ighalo, Biosorption of pollutants by plant leaves: An empirical review, Journal of Environmental, Chem. Eng. (2019).
[69] V.O. Arief, K. Trilestari, J. Sunarso, N. Indraswati, S. Ismadji, Recent progress on biosorption of heavy metals from liquids using low cost biosorbents: characterization, biosorption parameters and mechanism studies, CLEAN – Soil Air, Water 36 (2008) 937–962.
[70] W.S.W. Ngah, M.A.K.M. Hanafiah, Biosorption of copper ions from dilute aqueous solutions on base treatedrubber (Hevea brasiliensis) leaves powder: kinetics, isotherm, and biosorption mechanisms, J. Environ. Sci. 20 (2008) 1168–1176.
[71] S.S. Madaeni, H. Ahmadi Monfared, V. Vatanpour, A. Arabi Shamsabadi, E. Salehi, P. Daraei, S. Laki, S.M. Khatami, Coke removal from petrochemical oily wastewater using γ-Al2O3 based ceramic microfiltration membrane, Desalination 293 (2012) 87–93.
[72] M. Wakkel, B. Khiari, F. Zagrouba, Textile wastewater treatment by agro-industrial waste: Equilibrium modelling, thermodynamics and mass transfer mechanisms of cationic dyes adsorption onto low-cost lignocellulosic adsorbent, J. Taiwan Inst. Chem. Eng. 96 (2019) 439–452.